Supporting Information

AAO-Assisted Low-Cost Flexible Capacitive Pressure Sensors Based on Double-Sided Nanopillars by Facile Fabrication Method

*Yunjian Guo[1], Song Gao[1,2], Wenjing Yue[1,2], Chunwei Zhang[1,2], Yang Li[*1,2]*

[1] School of Information Science and Engineering, University of Jinan, Jinan 250022, China

[2] Shandong Provincial Key Laboratory of Network Based Intelligent Computing, University of Jinan, Jinan 250022, China

E-mail: ise_liy@ujn.edu.cn (Yang Li)

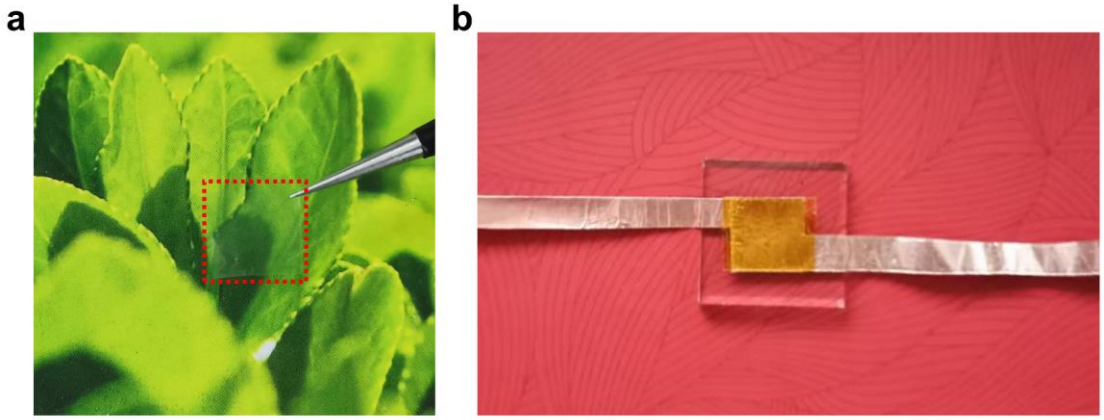

Figure S1. Photographs of (a) a P(VDF-TrFE) film with double-sided nanopillars (marked by a red dotted line) and (b) an assembled pressure sensor.

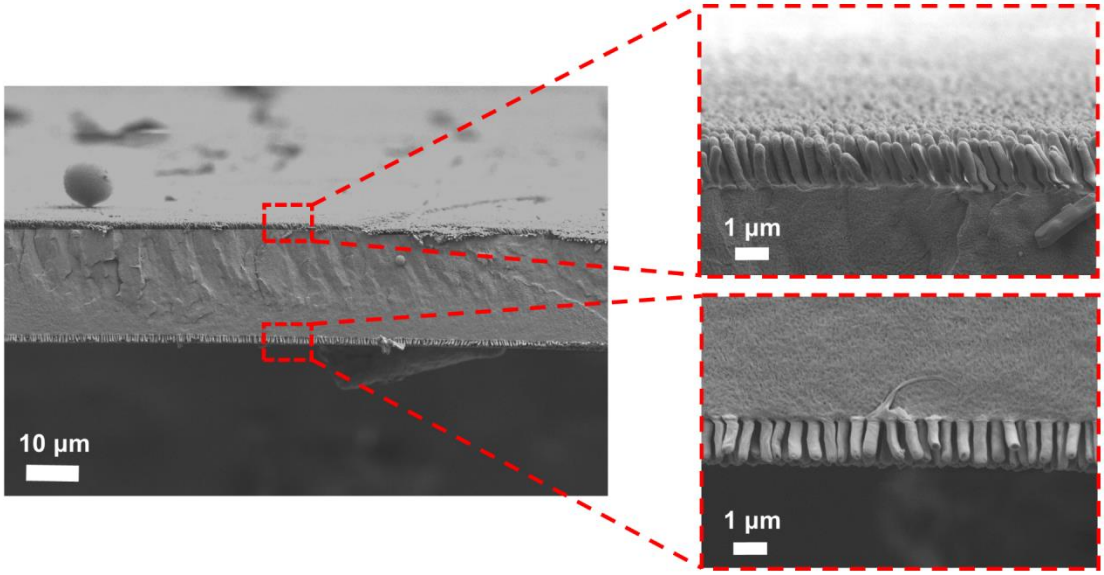

Figure S2. The cross-sectional SEM image and partially enlarged view of the double-sided nanopillars.

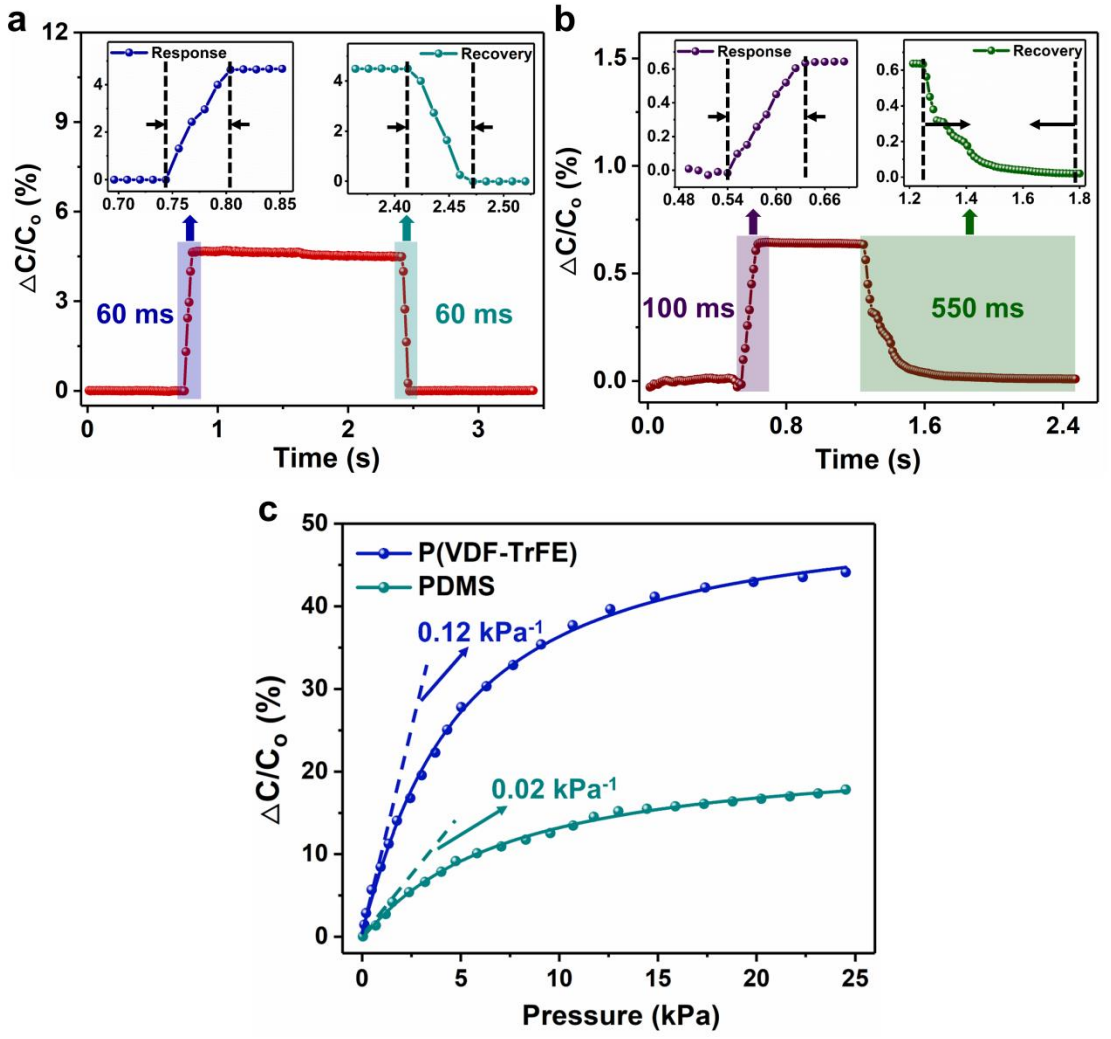

Figure S3. The response and recovery time when a pressure of 0.32 kPa is applied to (a) the P(VDF-TrFE)- and (b) the PDMS-based planar dielectric layer structured sensor, respectively. (c) The relative capacitance variation and sensitivity of the two sensors.

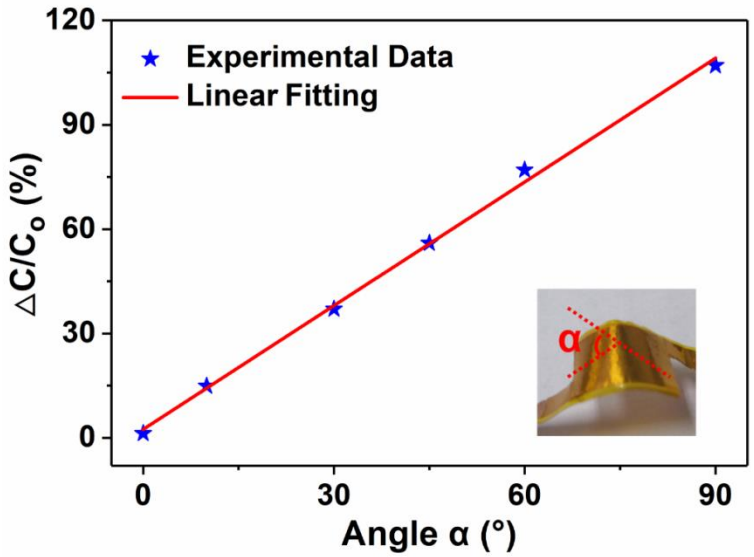

Figure S4. The relationship between the capacitance response and bending angle.

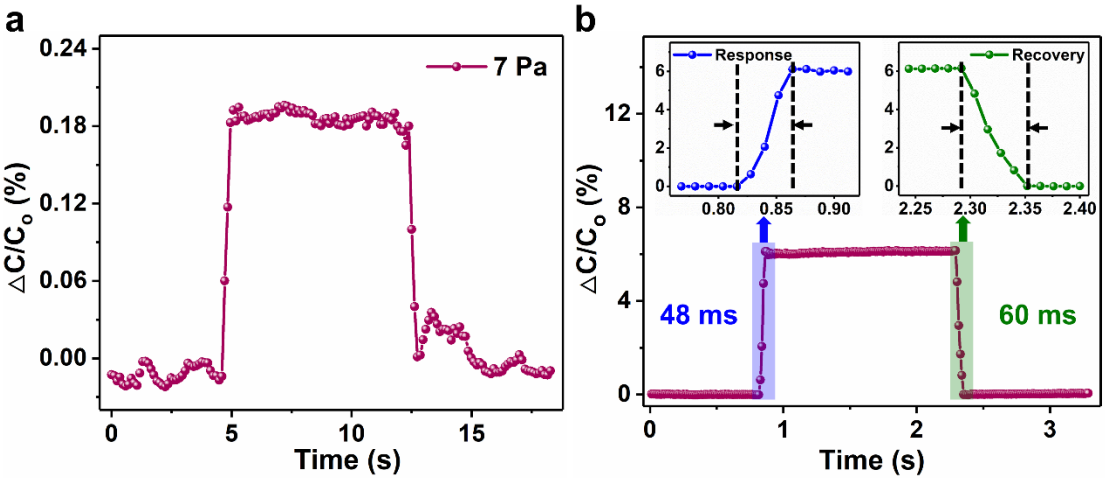

Figure S5. (a) Capacitance response by loading/unloading a slight paper (7 Pa) on the sensor based on single-sided nanopillars to measure the LOD. (b) The response and recovery time when a pressure of 0.32 kPa is applied to the sensor based on single-sided nanopillars.

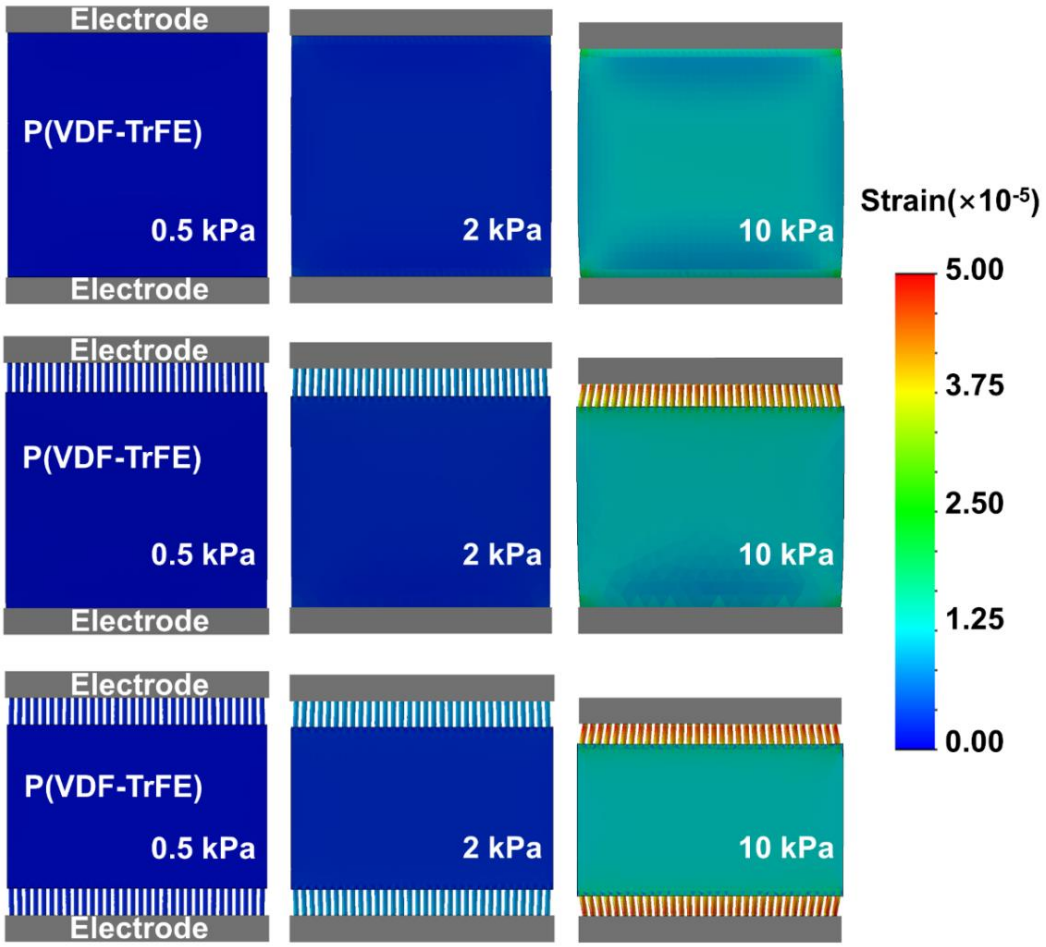

Figure S6. The strain distribution of three sensors under pressures of 0.5, 2, and 10 kPa, obtained by FEA simulation.

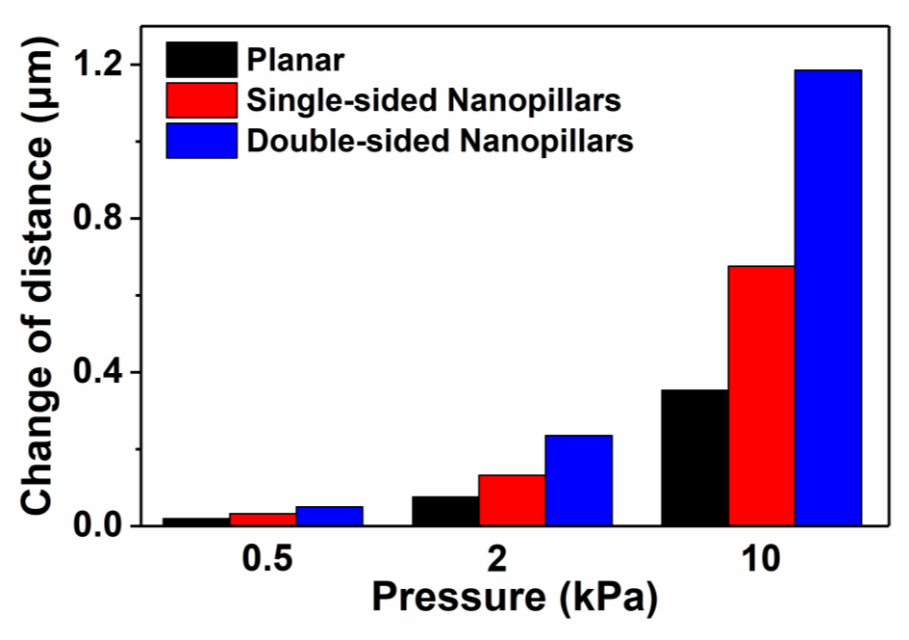

Figure S7. The quantified change of the separation distance under various pressures for each sensor obtained by FEA simulation.

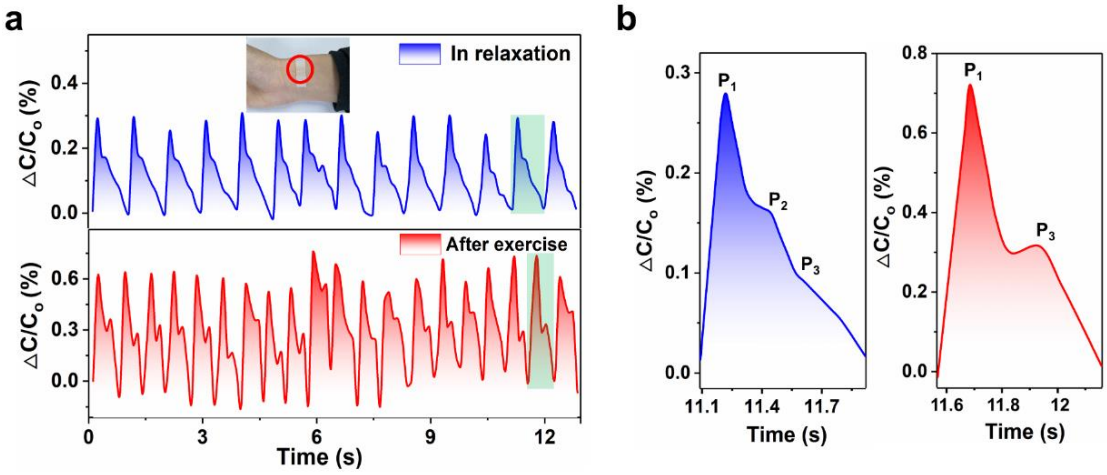

Figure S8. (a) Relative capacitance changes of the wrist pulse before and after exercise. (b)The magnified view of a single pulse before and after exercise, where three typical peaks marked as P_1, P_2 and P_3 correspond to the incident, tidal, and diastolic waves.

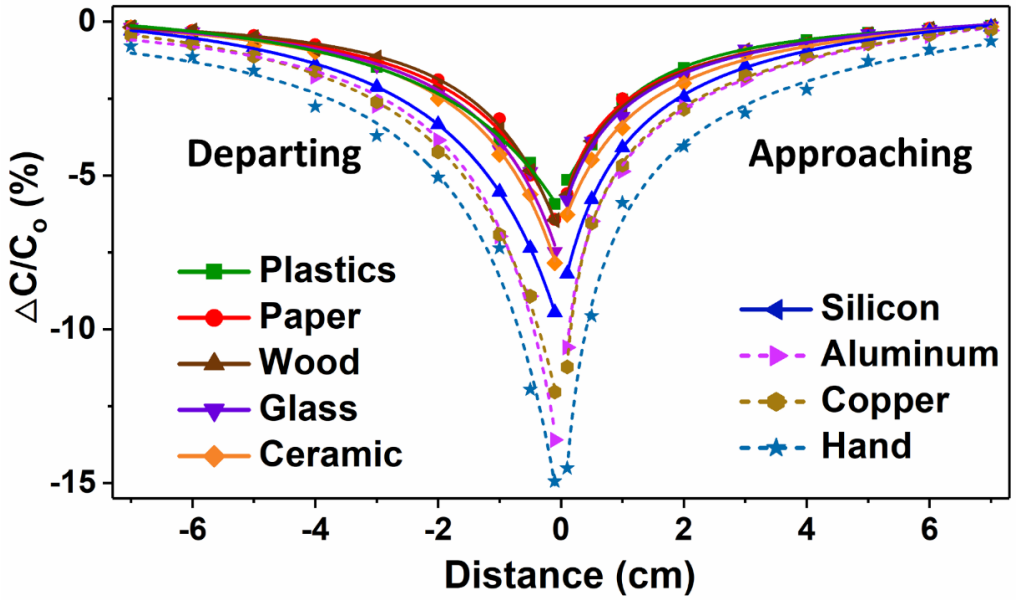

Figure S9. The capacitance responses when the object made of different materials approaching and departing the sensor at various distances.

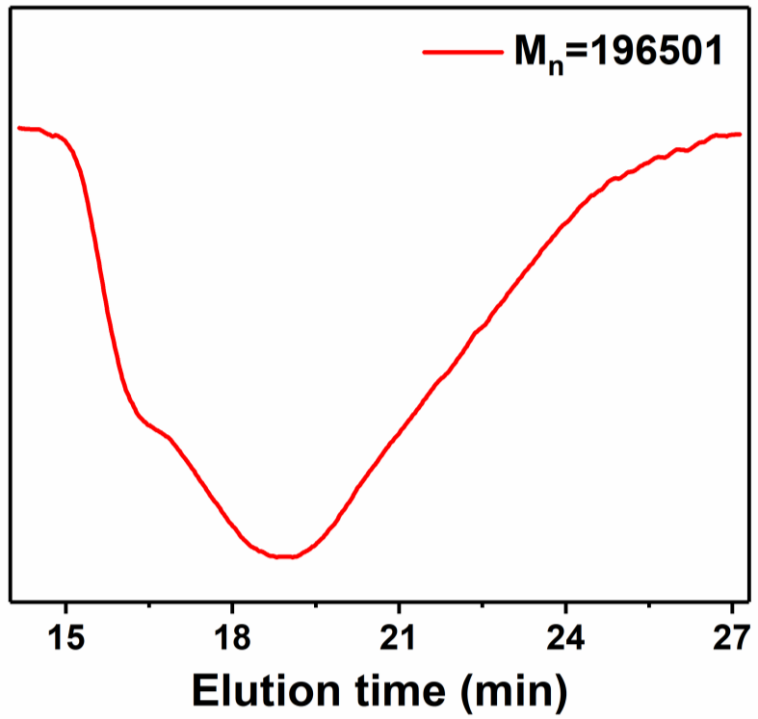

Figure S10. The GPC analysis of P(VDF-TrFE).

Detailed explanation of the letters in Figure 4a

In Figure 4a, ε_p, ε_s, ε_d, ε'_s and ε'_d stand for the dielectric constant of planar dielectric layer, single-sided nanopillars structured dielectric layer, double-sided nanopillars structured dielectric layer, single-sided nanopillars structured dielectric layer after pressing and double-sided nanopillars structured dielectric layer after pressing, respectively. d_p, d_s and d_d indicate the initial distance of planar dielectric layer, single-sided nanopillars structured dielectric layer and double-sided nanopillars structured dielectric layer, respectively. d'_p, d'_s and d'_d mean the changed distance of planar dielectric layer, single-sided nanopillars structured after pressing and double-sided nanopillars structured after pressing, respectively. $\triangle d_p$, $\triangle d_s$ and $\triangle d_d$ denote the distance variation of planar dielectric layer, single-sided nanopillars structured dielectric layer and double-sided nanopillars structured dielectric layer, respectively.

Table S1. Performance comparison of recent published works based on different flexible pressure sensors.

Sensing materials	**Types of devices**	**Sensitivity (testing pressure)**	**Working range**	**Response/ Recovery time**	**Cyclic stability**	**Ref**
Graphene	piezoresistivity	25.1 kPa^{-1}	16 Pa	120/80 ms	3000	1
rGO	piezoresistivity	178 kPa^{-1}	42 Pa	261/131 ms	1200	2
PZT	piezoelectricity	0.018 kPa^{-1}	–	60 ms	5000	3
P(VDF-TrFE), graphene	piezoelectricity	35 mA/Pa^{-1}	0.6 Pa	–	5000	4

PET, conductive fiber	triboelectricity	0.77 V kPa^{-1}	–	80 ms	5000	5
P(VDF-TrFE), PDMS	triboelectricity	0.55 V kPa^{-1}	–	–	10000	6
Air-Dielectric Graphene	transistor	2.05×10^{-4} kPa^{-1}	250 Pa–3 MPa	31/49 ms	–	7
Graphene	transistor	0.16 mm^{-1}	–	15 ms	>1000	8
PDMS	capacitance	0.42 kPa^{-1} (<1.5 kPa)	1 Pa	70 ms	1000	9
Eco-flex	capacitance	0.01887 kPa^{-1} (<45 kPa)	35 Pa–700 kPa	–	7200	10
Water-dilutable polyurethane acrylate	capacitance	0.61 kPa^{-1} (<1 kPa)	–	180/270 ms	10000	11
Polyethylene	capacitance	0.09 kPa^{-1} (<5 kPa)	–	–	–	12
Ecoflex	capacitance	0.0224 kPa^{-1} (<16 kPa)	7.3 Pa –360 kPa	–	–	13
PDMS	capacitance	0.6 kPa^{-1} (<1 kPa)	4.5 Pa	180/120 ms	2000	14
Ecoflex with air gap channels	capacitance	7.7×10^{-3} kPa^{-1} (<10 kPa)	-60 kPa–20 kPa	–	1000	15
PDMS	capacitance	0.171 kPa^{-1} (<5 kPa)	–	162 ms	1000	16
P(VDF-TrFE)	**capacitance**	**0.35 kPa^{-1} (<2 kPa)**	**4 Pa–25 kPa**	**48/60 ms**	**>3000**	**(this work)**

Table S2. GPC Results of P(VDF-TrFE).

M_n	M_w	M_p	M_z	M_{z+1}	M_z/M_w	M_{z+1}/M_w
196501	605096	485375	1392398	2148338	2.301119	3.550409

References

(1) Pang, Y.; Zhang, K.; Yang, Z.; Jiang, S.; Ju, Z.; Li, Y.; Wang, X.; Wang, D.; Jian, M.; Zhang, Y.; Liang, R.;Tian, H.;Yang, Y.; Ren, T. L. Epidermis Microstructure Inspired Graphene Pressure Sensor with Random Distributed Spinosum for High Sensitivity and Large Linearity. *ACS Nano* **2018**, *12*, 2346–2354.

(2) Jia, J.; Huang, G.; Deng, J.; Pan, K. Skin-Inspired Flexible and High-Sensitivity Pressure Sensors Based on RGO Films with Continuous-Gradient Wrinkles. *Nanoscale* **2019**, *11*, 4258–4266.

(3) Park, D. Y.; Joe, D. J.; Kim, D. H.; Park, H.; Han, J. H.; Jeong, C. K.; Park, H.; Park, J. G.; Joung, B.; Lee, K. J. Self-Powered Real-Time Arterial Pulse Monitoring Using Ultrathin Epidermal Piezoelectric Sensors. *Adv. Mater.* **2017**, *29*, 1702308.

(4) Park, J.; Kim, M.; Lee, Y.; Lee, H. S.; Ko, H. Fingertip Skin-Inspired Microstructured Ferroelectric Skins Discriminate Static/Dynamic Pressure and Temperature Stimuli. *Sci. Adv.* **2015**, *1*, e1500661.

(5) Lin, Z.; Yang, J.; Li, X.; Wu, Y.; Wei, W.; Liu, J.; Chen, J.; Yang, J. Large-Scale and Washable Smart Textiles Based on Triboelectric Nanogenerator Arrays for Self-Powered Sleeping Monitoring. *Adv. Funct. Mater.* **2018**, *28*, 1704112.

(6) Ha, M.; Lim, S.; Cho, S.; Lee, Y.; Na, S.; Baig, C.; Ko, H. Skin-Inspired Hierarchical Polymer Architectures with Gradient Stiffness for Spacer-Free, Ultrathin, and Highly Sensitive Triboelectric Sensors. *ACS Nano* **2018**, *12*, 3964–3974.

(7) Shin, S. H.; Ji, S.; Choi, S.; Pyo, K. H.; Wan An, B.; Park, J.; Kim, J.; Kim, J. Y.; Lee, K. S.; Kwon, S. Y.; Heo, J.; Park, B. G.; Park, J. U. Integrated Arrays of Air-Dielectric Graphene Transistors as Transparent Active-Matrix Pressure Sensors for Wide Pressure Ranges. *Nat. Commun.* **2017**, *8*, 14950.

(8) Meng, Y.; Zhao, J.; Yang, X.; Zhao, C.; Qin, S.; Cho, J. H.; Zhang, C.; Sun, Q.; Wang, Z. L. Mechanosensation-Active Matrix Based on Direct-Contact Tribotronic Planar Graphene Transistor Array. *ACS Nano* **2018**, *12*, 9381–9389.

(9) Luo, Y.; Shao, J.; Chen, S.; Chen, X.; Tian, H.; Li, X.; Wang, L.; Wang, D.; Lu, B. Flexible Capacitive Pressure Sensor Enhanced by Tilted Micropillar Arrays. *ACS Appl. Mater. Interfaces* **2019**, *11*, 17796–17803.

(10) Hou, C.; Xu, Z.; Qiu, W.; Wu, R.; Wang, Y.; Xu, Q.; Liu, X. Y.; Guo, W. A Biodegradable and Stretchable Protein-Based Sensor as Artificial Electronic Skin for Human Motion Detection. *Small* **2019**, *15*, 1805084.

(11) Yin, X.; Zhang, Y.; Xiao, J.; Moorlag, C.; Yang, J. Monolithic Dual-Material 3D Printing of Ionic Skins with Long-Term Performance Stability. *Adv. Funct. Mater.* **2019**, *29*, 1904716.

(12) Lei, Z.; Wu, P. Zwitterionic Skins with a Wide Scope of Customizable Functionalities. *ACS Nano* **2018**, *12*, 12860–12868.

(13) Hua, Q.; Sun, J.; Liu, H.; Bao, R.; Yu, R.; Zhai, J.; Pan, C.; Wang, Z. L. Skin-Inspired Highly Stretchable and Conformable Matrix Networks for Multifunctional Sensing. *Nat. Commun.* **2018**, *9*, 244.

(14) Liu, Y.-Q.; Zhang, J.-R.; Han, D.-D.; Zhang, Y.-L.; Sun, H.-B. Versatile Electronic Skins with Biomimetic Micronanostructures Fabricated Using Natural Reed Leaves as Templates. *ACS Appl. Mater. Interfaces* **2019**, *11*, 38084–38091.

(15) Shi, H.; Al-Rubaiai, M.; Holbrook, C. M.; Miao, J.; Pinto, T.; Wang, C.; Tan, X. Screen-Printed Soft Capacitive Sensors for Spatial Mapping of Both Positive and Negative Pressures. *Adv. Funct. Mater.* **2019**, *29*, 1903020.

(16) Wang, J.; Suzuki, R.; Shao, M.; Gillot, F.; Shiratori, S. Capacitive Pressure Sensor with Wide-Range, Bendable, and High Sensitivity Based on the Bionic Komochi Konbu Structure and Cu/Ni Nanofiber Network. *ACS Appl. Mater. Interfaces* **2019**, *11*, 11928–11935.